

Measurement of polarization charge and conduction-band offset at $\text{In}_x\text{Ga}_{1-x}\text{N}/\text{GaN}$ heterojunction interfaces

H. Zhang, E. J. Miller, and E. T. Yu^{a)}

Department of Electrical and Computer Engineering, University of California at San Diego, La Jolla, California 92093-0407

C. Poblenz and J. S. Speck

Materials Department, University of California at Santa Barbara, Santa Barbara, California 93106

(Received 4 February 2004; accepted 9 April 2004; published online 19 May 2004)

The spontaneous and piezoelectric polarization fields in group-III nitride semiconductors lead to the presence of large electrostatic sheet charge densities at nitride semiconductor heterojunction interfaces. Precise quantitative knowledge of these polarization-induced charge densities and of the band-edge discontinuities at nitride heterojunction interfaces is therefore essential in nitride semiconductor device design and analysis. We have used capacitance–voltage profiling to measure the conduction-band offset and polarization charge density at $\text{In}_x\text{Ga}_{1-x}\text{N}/\text{GaN}$ heterojunction interfaces with $x=0.054$ and $x=0.09$. We obtain conduction-band offsets $\Delta E_C=0.09\pm 0.07$ eV for $x=0.054$ and $\Delta E_C=0.22\pm 0.05$ eV for $x=0.09$, corresponding to an averaged conduction-to-valence-band offset ratio $\Delta E_C:\Delta E_V$ of 58:42. Our measurements yield polarization charge densities of $(1.80\pm 0.32)\times 10^{12}$ e/cm² for $x=0.054$ and $(4.38\pm 0.36)\times 10^{12}$ e/cm² for $x=0.09$. These values are smaller than those predicted by recent theoretical calculations, but in good agreement with values inferred from a number of optical experiments. © 2004 American Institute of Physics. [DOI: 10.1063/1.1759388]

Group III-nitride semiconductor heterostructures have attracted intense interest for both electronic and optoelectronic device applications, with $\text{In}_x\text{Ga}_{1-x}\text{N}/\text{GaN}$ heterostructures being of particular interest for visible light emitters¹ and for electronic devices such as heterojunction bipolar transistors.^{2,3} The large polarization charge densities present at group III-nitride semiconductor heterojunction interfaces^{4,5} profoundly influence electric field and mobile carrier distributions, necessitating their incorporation into device design and analysis and providing opportunities for device engineering. Accurate knowledge of these charge densities as well as of the heterojunction band offsets is therefore essential for proper device modeling and design. While the evaluation of polarization charge densities at the $\text{In}_x\text{Ga}_{1-x}\text{N}/\text{GaN}$ interface^{4,6} has been pursued quite effectively, considerably less definitive information is available about polarization charge densities and band offsets at the $\text{In}_x\text{Ga}_{1-x}\text{N}/\text{GaN}$ interface.

We have used capacitance–voltage (C – V) profiling to measure both the polarization charge density and the conduction-band offset at the $\text{In}_x\text{Ga}_{1-x}\text{N}/\text{GaN}$ interface. The epitaxial layer structure of the $\text{In}_x\text{Ga}_{1-x}\text{N}/\text{GaN}$ samples used in this study is shown schematically in Fig. 1, along with the computed energy-band-edge diagram for the $\text{In}_{0.09}\text{Ga}_{0.91}\text{N}/\text{GaN}$ sample and a plot of the corresponding electrostatic charge density. The positive polarization charge at the upper $\text{In}_x\text{Ga}_{1-x}\text{N}/\text{GaN}$ interface leads to electron accumulation in the $\text{In}_x\text{Ga}_{1-x}\text{N}$ layer, while the negative polarization charge at the lower $\text{In}_x\text{Ga}_{1-x}\text{N}/\text{GaN}$ interface causes formation of a depletion layer with charge density qN_d^+ sur-

rounding the interface. Two samples were characterized, one with a 30 nm $\text{In}_{0.054}\text{Ga}_{0.946}\text{N}$ layer and the other with a 50 nm $\text{In}_{0.09}\text{Ga}_{0.91}\text{N}$ layer. Both samples were grown by rf-plasma assisted molecular-beam epitaxy (MBE) on a ~ 1.5 μm thick metal organic chemical vapor deposition GaN template deposited on a sapphire substrate.⁷ The MBE epitaxial layers were grown at 650 °C and the crystal polarity was determined to be Ga face, based on cross-sectional transmission electron microscopy and atomic force microscopy measurements. X-ray reciprocal space mapping measurements were used to determine the composition of the $\text{In}_x\text{Ga}_{1-x}\text{N}$ layers and to confirm that the heterostructures were fully strained. To minimize Schottky diode leakage currents in the $\text{In}_{0.09}\text{Ga}_{0.91}\text{N}$ sample, a thin layer of silicon oxide (30–130

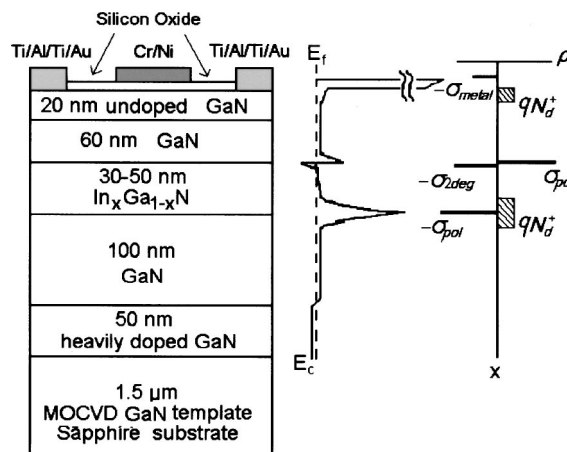


FIG. 1. Schematic diagram of the $\text{In}_x\text{Ga}_{1-x}\text{N}/\text{GaN}$ epitaxial layer structure and the corresponding energy-band-edge diagram and electrostatic charge distribution.

^{a)}Electronic mail: ety@ece.ucsd.edu

Å) was first grown by plasma-enhanced chemical vapor deposition (PECVD) to reduce the flow of leakage current. To minimize the oxide–GaN interface state density,⁸ the samples were first cleaned in organic solvents and then soaked in an NH₄OH solution at 50 °C for 15 min. An N₂ plasma treatment was performed at 300 °C with an excitation power of 30 W for 5 min immediately before oxide deposition in the same chamber at a lower temperature. This layer of oxide effectively reduced the reverse leakage current by 1 to 2 orders of magnitude, enabling accurate *C*–*V* characterization. The effect of the oxide layer on the measured capacitance can be accounted for by considering the oxide capacitance to be in series with that of the semiconductor. Buffered oxide etch was used to remove the PECVD-grown oxide in the ohmic contact region prior to ohmic metal deposition. Ti/Al/Ti/Au (330 Å/770 Å/300 Å/1000 Å) ohmic contact metallization was deposited using electron-beam evaporation and then annealed in forming gas at 650 °C for 1 min. Cr/Ni (200 Å/1200 Å) metallization was used for the Schottky contact, with Cr serving to enhance the adhesion of Ni to the oxide layer. For the In_{0.054}Ga_{0.946}N sample, the leakage current was small enough to allow accurate *C*–*V* profiling without oxide deposition. Ti/Al/Ti/Au ohmic contacts annealed at 650 °C were fabricated as described above, and 1500 Å Ni Schottky contacts were directly evaporated on the nitride sample surface.

C–*V* measurements were performed using an HP 4285A Precision LCR meter at frequencies ranging from 100 kHz to 3 MHz, at room temperature under ambient lighting conditions. Electrical data were acquired in the parallel circuit mode of the HP4285A, yielding capacitance and conductance *C_p* and *G_p*, respectively. The Schottky diode was modeled using an equivalent circuit consisting of a junction capacitance *C* and a junction conductance *G* in parallel combined with a series resistance *r_s*.⁹ The measured quantities *C_p* and *G_p* are related to *C*, *G*, and *r_s* according to

$$\frac{G^2}{C} + \omega^2 C = \frac{G_p^2}{C_p} + \omega^2 C_p, \quad (1)$$

$$\frac{G}{G^2 + (\omega C)^2} + r_s = \frac{G_p}{G_p^2 + (\omega C_p)^2}, \quad (2)$$

where *r_s* is determined from the measured *G_p* under large forward bias, when 1/*G* becomes comparatively small and 1/*G_p* therefore approximates *r_s*.

The apparent carrier distribution *n*^{*} and depletion width *w* are then given by⁹

$$n^* = -\frac{2}{q\epsilon S^2 d(1/C^2)/dV}, \quad (3)$$

$$w = \frac{\epsilon S}{C}, \quad (4)$$

where *q* is the electronic charge, ϵ is the dielectric constant of the semiconductor material, and *S* is the area under the Schottky contact. The interface charge density *Q_i* and the conduction-band offset ΔE_C at the heterojunction interface can be calculated using the following expressions:¹⁰

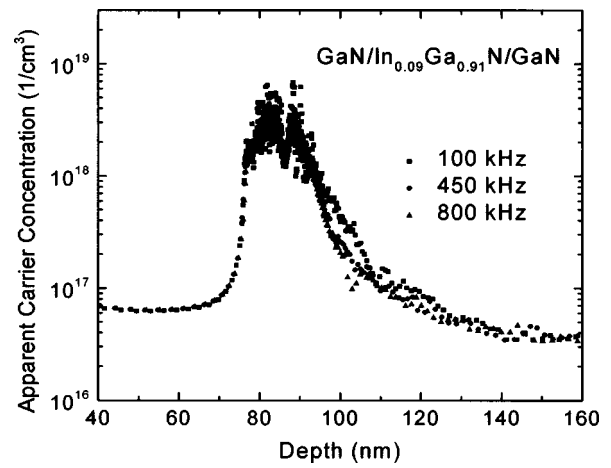


FIG. 2. Apparent carrier concentration profiles for the In_{0.09}Ga_{0.91}N/GaN heterostructure, derived from *C*–*V* data obtained at frequencies of 100 kHz, 450 kHz, and 800 kHz.

$$Q_i = q \int_{w_1}^{w_2} (n^*(w) - N_d^+(w)) dw, \quad (5)$$

$$\Delta E_C = -q^2 \int_{w_1}^{w_2} \left\{ \frac{1}{\epsilon(w)} [N_d^+(w) - n^*(w)] (w - w_h) \right\} dw - kT \left[\ln \left(\frac{n_1/N_{C1}}{n_2/N_{C2}} \right) + \frac{1}{\sqrt{8}} \left(\frac{n_1}{N_{C1}} - \frac{n_2}{N_{C2}} \right) \right], \quad (6)$$

where $N_d^+(w)$ is the ionized donor concentration at a distance *w* from the metal/semiconductor interface, *N_{C1}* and *N_{C2}* are the conduction-band effective densities of states of the first and the second layers of semiconductor material, respectively, *n₁* and *n₂* are the free electron densities in the corresponding layers, *w_h* is the heterojunction position, and *k* is Boltzmann's constant. The integration limits *w₁* and *w₂* are chosen to be far from the heterojunction, where the electric field is negligible.

Typical apparent carrier concentration profiles obtained using Eqs. (3) and (4) for the GaN/In_{0.09}Ga_{0.91}N/GaN heterostructure are shown in Fig. 2. Qualitatively similar carrier concentration profiles were obtained for the GaN/In_{0.054}Ga_{0.946}N/GaN heterostructure. Equations (5) and (6) were then used to calculate the band offset and polarization charge densities based on this carrier distribution. By analyzing data acquired at measurement frequencies varying from 100 kHz to 800 kHz from several different diodes, we have determined the conduction-band offsets to be $\Delta E_C = 0.09 \pm 0.07$ eV and $\Delta E_C = 0.22 \pm 0.05$ eV for GaN/In_{*x*}Ga_{1–*x*}N heterojunctions with *x*=0.054 and *x*=0.09, respectively. Based on the energy band gaps of 3.42 eV for GaN, 3.225 eV for In_{0.054}Ga_{0.946}N, and 3.06 eV for In_{0.09}Ga_{0.91}N (Refs. 11 and 12) coherently strained to GaN, and based on the experimental uncertainties for each measurement, we deduce a weighted average of the band offset ratio $\Delta E_C : \Delta E_V$ of 58:42. In comparison, an analysis of deep yellow photoluminescence (PL) in GaN and In_{*x*}Ga_{1–*x*}N alloys yielded¹³ estimates for ΔE_C of 0.11 eV and 0.18 eV (Ref. 13) for *x*=0.054 and *x*=0.09, respectively while a *C*–*V* analysis¹⁴ of a *p*–In_{*x*}Ga_{1–*x*}N/*n*–GaN diode to obtain

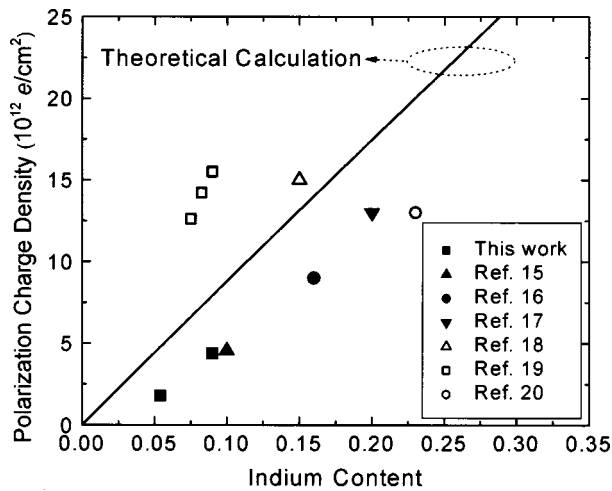


FIG. 3. $\text{In}_x\text{Ga}_{1-x}\text{N}/\text{GaN}$ polarization charge densities from this work (■), and inferred from Ref. 15 (▲), Ref. 16 (●), Ref. 17 (▼), Ref. 18 (△), Ref. 19 (□), and Ref. 20 (○). Calculated polarization charge densities (Ref. 4) are also shown.

the valence-band offset, ΔE_V , implies conduction-band offsets of 0.13 eV and 0.22 eV for the $\text{In}_{0.054}\text{Ga}_{0.946}\text{N}/\text{GaN}$ and $\text{In}_{0.09}\text{Ga}_{0.91}\text{N}/\text{GaN}$ interfaces, respectively.

The polarization charge densities at the $\text{In}_{0.054}\text{Ga}_{0.946}\text{N}/\text{GaN}$ and $\text{In}_{0.09}\text{Ga}_{0.91}\text{N}/\text{GaN}$ interfaces deduced from our measurements are $(1.80 \pm 0.32) \times 10^{12} \text{ e/cm}^2$ and $(4.38 \pm 0.36) \times 10^{12} \text{ e/cm}^2$. In comparison, theoretical calculations yield substantially higher values ranging from 4.43×10^{12} to $5.25 \times 10^{12} \text{ e/cm}^2$ for $x=0.054$ and from 6.84×10^{12} to $8.74 \times 10^{12} \text{ e/cm}^2$ for $x=0.09$, depending on the different elastic, piezoelectric, and lattice constants available.⁴ Although few direct measurements of the $\text{In}_x\text{Ga}_{1-x}\text{N}/\text{GaN}$ interface polarization charge densities are readily available for comparison, polarization charge densities can be inferred from values of the electric-field magnitude within $\text{In}_x\text{Ga}_{1-x}\text{N}/\text{GaN}$ quantum well structures deduced from PL,^{15–18} electroabsorption,¹⁹ and electrotransmission²⁰ experiments. Because of the polarization charges present at each heterojunction interface, a large internal electric field is induced within an $\text{In}_x\text{Ga}_{1-x}\text{N}/\text{GaN}$ quantum well. Due to carrier screening effects, however, determination of the polarization charge density corresponding to a reported value for the electric field requires a self-consistent solution of the Poisson–Schrödinger equations for the full quantum well structure. Thus, by assuming the quantum well structure to be known *a priori* and taking the polarization charge density at the heterostructure interface as a variable parameter, we have used a one-dimensional (1D) Poisson/Schrödinger solver²¹ to compute the electric field as a function of polarization charge density. By adjusting the polarization charge density until good agreement is achieved between the simulated and optically measured values of the electric field, the polarization charge density, shown in Fig. 3, can be inferred. From Fig. 3, we see that the majority of measurements yield polarization charge densities somewhat

lower than those predicted theoretically, and in good agreement with our measured values. Further investigations are needed to determine the origin of the large range of values reported for polarization charge density at the $\text{In}_x\text{Ga}_{1-x}\text{N}/\text{GaN}$ interface.

In summary, $C-V$ profiling has been used to measure the polarization charge densities and conduction-band offsets in $\text{In}_{0.054}\text{Ga}_{0.946}\text{N}/\text{GaN}$ and $\text{In}_{0.09}\text{Ga}_{0.91}\text{N}/\text{GaN}$ heterostructures. We obtain conduction-band offsets of $0.09 \pm 0.07 \text{ eV}$ and $0.22 \pm 0.05 \text{ eV}$ respectively, corresponding to a band offset ratio $\Delta E_C : \Delta E_V$ of 58:42. The polarization charge densities at the interfaces are $(1.80 \pm 0.32) \times 10^{12} \text{ e/cm}^2$ and $(4.38 \pm 0.36) \times 10^{12} \text{ e/cm}^2$ for $\text{In}_{0.054}\text{Ga}_{0.946}\text{N}/\text{GaN}$ and $\text{In}_{0.09}\text{Ga}_{0.91}\text{N}/\text{GaN}$ heterojunctions, respectively, smaller than the theoretical predictions but in good agreement with values inferred from a substantial body of optical data.

Part of this work was supported by ONR (POLARIS MURI, monitored by Dr. Colin Wood).

- ¹S. Nakamura and G. Fasol, *The Blue Laser Diode* (Springer, Berlin, 1997).
- ²T. Makimoto, K. Kumakura, and N. Kobayashi, *Appl. Phys. Lett.* **83**, 1035 (2003).
- ³S. N. Mohammad and H. Morkoc, *J. Appl. Phys.* **78**, 4200 (1995).
- ⁴O. Ambacher, J. Majewski, C. Miskys, A. Link, M. Hermann, M. Eickhoff, M. Stutzmann, F. Bernardini, V. Fiorentini, V. Tilak, B. Schaff, and L. F. Eastman, *J. Phys.: Condens. Matter* **14**, 3399 (2002).
- ⁵E. T. Yu, G. J. Sullivan, P. M. Asbeck, C. D. Wang, D. Qiao, and S. S. Lau, *Appl. Phys. Lett.* **71**, 2794 (1997).
- ⁶E. J. Miller, E. T. Yu, C. Poblenz, C. Elsass, and J. S. Speck, *Appl. Phys. Lett.* **18**, 3551 (2002).
- ⁷C. Poblenz, T. Mates, M. Craven, S. P. DenBaars, and J. S. Speck, *Appl. Phys. Lett.* **81**, 2767 (2002).
- ⁸R. Nakasaki, T. Hashizume, and H. Hasegawa, *Physica E (Amsterdam)* **7**, 953 (2000).
- ⁹D. Schroder, *Semiconductor Material and Device Characterization*, 2nd ed. (Wiley, Toronto, 1998).
- ¹⁰H. Kroemer, W.-Y. Chien, J. S. Harris, and D. D. Edwall, *Appl. Phys. Lett.* **36**, 295 (1980).
- ¹¹L. T. Romano, B. S. Krusor, M. D. McCluskey, and D. P. Bour, *Appl. Phys. Lett.* **73**, 1757 (1998).
- ¹²C. Wetzel, T. Takeuchi, S. Yamaguchi, H. Katoh, H. Amano, and I. Akasaki, *Appl. Phys. Lett.* **73**, 1994 (1998).
- ¹³C. Manz, M. Kunzer, H. Obloh, A. Ramakrishnan, and U. Kaufmann, *Appl. Phys. Lett.* **74**, 3993 (1999).
- ¹⁴T. Makimoto, K. Kumakura, T. Nishida, and N. Kobayashi, *J. Electron. Mater.* **31**, 313 (2002).
- ¹⁵S. F. Chichibu, A. C. Abare, M. S. Minsky, S. Keller, S. B. Fleischer, J. E. Bowers, E. Hu, U. K. Mishra, L. A. Coldren, and S. P. DenBaars, and T. Sota, *Appl. Phys. Lett.* **73**, 2006 (1998).
- ¹⁶T. Takeuchi, C. Wetzel, S. Yamaguchi, H. Sakai, H. Amano, I. Akasaki, Y. Kaneko, S. Nakagawa, Y. Yamaoka, and N. Yamada, *Appl. Phys. Lett.* **73**, 1691 (1998).
- ¹⁷P. Lefebvre, A. Morel, M. Gallart, T. Taliércio, J. Allègre, B. Gil, H. Mathieu, B. Damilano, N. Grandjean, and J. Massies, *Appl. Phys. Lett.* **78**, 1252 (2001).
- ¹⁸Y. D. Jho, J. S. Yahng, E. Oh, and D. S. Kim, *Appl. Phys. Lett.* **79**, 1130 (2001).
- ¹⁹F. Renner, P. Kiesel, and G. H. Döhler, M. Kneissl, C. G. Van de Walle, and N. M. Johnson, *Appl. Phys. Lett.* **81**, 490 (2002).
- ²⁰C. Y. Lai, T. M. Hsu, W.-H. Chang, and K.-U. Tseng, *J. Appl. Phys.* **91**, 531 (2002).
- ²¹G. L. Snider, *Computer Program 1D Poisson/Schrödinger: A Band Diagram Calculator* (University of Notre Dame, Notre Dame, IN, 1995).